

# Altered proteasome function in right ventricular hypertrophy

Tanja Heitmeier<sup>1‡</sup>, Akylbek Sydykov<sup>1‡</sup>, Christina Lukas<sup>2‡</sup>, Christina Vroom<sup>1‡</sup>, Martina Korfei<sup>1‡</sup>, Aleksandar Petrovic<sup>1‡</sup>, Karin Klingel<sup>3</sup>, Andreas Günther<sup>1,4‡</sup>, Oliver Eickelberg<sup>2,5‡</sup>, Norbert Weissmann<sup>1‡</sup>, Hossein Ardeschir Ghofrani<sup>1‡</sup>, Werner Seeger<sup>1,6‡</sup>, Friedrich Grimminger<sup>1‡</sup>, Ralph Theo Schermuly<sup>1\*†‡</sup>, Silke Meiners<sup>2\*†‡</sup>, and Djuro Kosanovic<sup>1,7†‡</sup>

<sup>1</sup>Universities of Giessen and Marburg Lung Center (UGMLC), Aulweg 130, 35392 Giessen, Germany; <sup>2</sup>Comprehensive Pneumology Center (CPC), University Hospital, Ludwig-Maximilians-University and Helmholtz Zentrum München, Max-Lebsche-Platz 31, 81377 Munich, Germany; <sup>3</sup>Institute for Pathology and Neuropathology, University of Tübingen, Germany; <sup>4</sup>Agaplesion Lung Clinic Waldhof Elgershausen, Greifenstein, Germany; <sup>5</sup>University of Colorado at Denver - Anschutz Medical Campus, 129263, Pulmonary and Critical Care Medicine University, Denver, CO, USA; <sup>6</sup>Max-Planck-Institute for Heart and Lung Research, Bad Nauheim, Germany; and <sup>7</sup>Sechenov First Moscow State Medical University (Sechenov University), Moscow, Russia

Received 29 November 2018; revised 1 February 2019; editorial decision 6 April 2019; accepted 16 April 2019

Time for primary review: 26 days

## Aims

In patients with pulmonary hypertension, right ventricular hypertrophy (RVH) is a detrimental condition that ultimately results in right heart failure and death. The ubiquitin proteasome system has been identified as a major protein degradation system to regulate cardiac remodelling in the left heart. Its role in right heart hypertrophy, however, is still ambiguous.

## Methods and results

RVH was induced in mice by pulmonary artery banding (PAB). Both, expression and activity of the proteasome was found to be up-regulated in the hypertrophied right ventricle (RV) compared to healthy controls. Catalytic inhibition of the proteasome by the two proteasome inhibitors Bortezomib (BTZ) and ONX-0912 partially improved RVH both in preventive and therapeutic applications. Native gel analysis revealed that specifically the 26S proteasome complexes were activated in experimental RVH. Increased assembly of 26S proteasomes was accompanied by elevated expression of Rpn6, a rate-limiting subunit of 26S proteasome assembly, in hypertrophied cardiomyocytes of the right heart. Intriguingly, patients with RVH also showed increased expression of Rpn6 in hypertrophied cardiomyocytes of the RV as identified by immunohistochemical staining.

## Conclusion

Our data demonstrate that alterations in expression and activity of proteasomal subunits play a critical role in the development of RVH. Moreover, this study provides an improved understanding on the selective activation of the 26S proteasome in RVH that might be driven by the rate-limiting subunit Rpn6. In RVH, Rpn6 therefore represents a more specific target to interfere with proteasome function than the commonly used catalytic proteasome inhibitors.

## Keywords

Proteasome • Proteasome inhibition • Rpn6 • Pulmonary artery banding • Right ventricular hypertrophy

## 1. Introduction

Right ventricular hypertrophy (RVH) is of important prognostic value for the outcome of patients with pulmonary hypertension (PH)<sup>1</sup> and several cardiomyopathies.<sup>2</sup> Although there are different causes of PH, they all

share the pathological feature of alterations in the pulmonary vasculature (remodelling)<sup>3</sup> which causes elevated pulmonary arterial pressure. The right ventricle (RV) adapts to this increased afterload with hypertrophy (Cor pulmonale).<sup>4</sup> With progression of the disease, the adaptive hypertrophy of the myocardium shifts to a maladaptive state of cardiac

\* Corresponding authors. Tel: +49 641 99 42420; fax: +49 641 99 42419, E-mail: ralph.schermuly@innere.med.uni-giessen.de (R.T.S.); Tel: +49 89 3187 4673; E-mail: silke.meiners@helmholtz-muenchen.de (S.M.)

† These authors contributed equally to this work.

‡ Members of the German Center for Lung Research (DZL).

remodelling. A pathological hallmark is the appearance of cardiac fibrosis.<sup>4</sup> The change in tissue structure, namely increased size of cardiomyocytes and overproduction of extracellular matrix, subsequently alters conduction of electric signals and the mechanical function of the heart. Eventually, this results in right heart failure (RHF)<sup>5</sup> which represents one of the most common causes of death in patients with PH.<sup>6</sup> Standard therapies in left heart diseases have so far failed to improve RV maladaptive remodelling.<sup>7</sup> In conclusion, there is an urgent need for new therapeutic strategies to target RV dysfunction by preventing or reversing cardiac remodelling.

One hallmark of cardiomyocyte hypertrophy is altered protein homeostasis that involves an overall increase in protein synthesis but also in protein degradation.<sup>8</sup> The ubiquitin–proteasome system is the major systems for intracellular protein degradation.<sup>9</sup> For that, proteins are first tagged with polyubiquitin chains and later degraded by the 26S proteasome. The protein degrading proteasome consists of a 20S catalytic core and one (26S proteasome) or two (30S proteasome) 19S regulatory caps. The 20S catalytic core forms a barrel that comprises three catalytic active sites. In a caspase-, trypsin-, or chymotrypsin-like manner (C-L, T-L, or CT-L), the catalytic subunits  $\beta 1$ ,  $\beta 2$ , and  $\beta 5$  cleave the target proteins after acidic, basic or hydrophobic amino acids, respectively.<sup>10</sup> Proteasome activators bind to the 20S catalytic core and facilitate opening of its—usually closed—pores, and allow substrate entry.<sup>11</sup> Among the known five proteasome activators, the 19S regulator (also called PA700) mediates ATP-dependent degradation of ubiquitin-tagged proteins.<sup>12</sup> The 19S proteasome is involved in the recognition and binding of the protein substrate to funnel it into the, now opened, 20S core.<sup>13</sup>

The ubiquitin–proteasome system is critically involved in numerous cellular processes such as cell cycle control, transcriptional regulation, stress and immune responses, and disposal of misfolded proteins.<sup>14</sup> It has been found dysregulated in numerous diseases including cancer, inflammation, fibrosis, PH, and cardiomyopathies.<sup>15</sup> The 26S proteasome has been comprehensively analysed by proteomic analyses in samples of whole hearts.<sup>16</sup> Proteasome expression and activity was differentially regulated in hypertrophic vs. failing hearts; while proteasome function was found to be up-regulated in experimental left ventricular hypertrophy (LVH) and dilative cardiomyopathy in patients, proteasome activity was impaired in failing left hearts.<sup>17</sup> Specific catalytic proteasome inhibitors have been applied in different experimental models of LVH where it successfully counteracted development and also reversed established LVH.<sup>18</sup> However, proteasome inhibitors accelerated progression to heart failure in experimental models of left heart failure.<sup>19,20</sup> Similarly, they have recently been tested in experimental models of RVH and RHF with controversial results; while the proteasome inhibitor bortezomib (BTZ) alleviated RVH,<sup>21</sup> proteasome inhibition partially augmented RHF.<sup>22</sup>

In this study, we identify the activation of the proteasome as a contributing factor to development and maintenance of RVH. Specifically, we observed activation of the 26S proteasome and overexpression of the 19S subunit Rpn6 in experimental RVH and in right hearts of patients with PH. These data identify Rpn6 as a novel potential target to specifically interfere with 26S proteasome activation in RVH.

## 2. Methods

For details on the immunohistochemical, protein, activity, and RNA analyses of mouse and human tissue, the reader is referred to the [Supplementary material online](#).

### 2.1 In vivo studies

All animal experiments were approved by the local ethics committee of the Regierungspraesidium Giessen and were performed conform the guidelines from Directive 2010/63/EU of the European Parliament on the protection of animals used for scientific purposes. The pulmonary artery banding (PAB) surgery to provoke RVH, echocardiographic assessments, and haemodynamic measurements were performed as reported previously.<sup>23</sup> The proteasome inhibitors BTZ [dose: 0.5 mg/kg body weight (BW)] and ONX-0912 (dose: 50 mg/kg BW) were used for preventive (*BTZ<sub>prev</sub>* and *ONX<sub>prev</sub>*) and therapeutic treatment (*BTZ<sub>ther</sub>* and *ONX<sub>ther</sub>*) ([Supplementary material online, Figure S1](#)). Three weeks after PAB, the mice were sacrificed and histology and protein/mRNA analysis were performed for various targets in RV tissue. For profound details of the model, drugs and molecular analyses the reader is referred to the [Supplementary material online](#).

### 2.2 Anaesthesia, analgesia, and euthanasia

The below described general anaesthesia via inhalation was used for echocardiography, PAB surgery, and haemodynamic measurements. First, the mouse was placed for about 5 min into an induction chamber where it was exposed to a mix of 5% isoflurane and 100% oxygen (Vetequip inhalation anaesthesia system SN: 3470). Once the righting and the pinch-toe reflexes were negative, the mouse was placed supine on the corresponding examining table. Next dexpanthenol was placed onto the eyes to avoid their dehydration. A rectal probe recorded the body temperature which was maintained at 37°C by a warming plate. Together with chest movement and pinch-toe reflex these parameters served as anaesthetic monitoring. Anaesthesia was maintained with 2.0% isoflurane-oxygen mix, delivered either by nose cone (echocardiography, haemodynamic measurements) or via tracheal tube (PAB surgery). Ventilation was carried out at 120–150/min, a breath volume of 200–250  $\mu$ L and 2 L flow. PAB surgery was performed to provoke RVH by reducing the cross-sectional area (CSA) of the artery to 0.3 mm (about 66% of original CSA). Briefly, a titanium clip was placed around the pulmonary trunk. In the case of the sham group, the same procedure was performed without placing a titanium clip. After PAB surgery, isoflurane was turned off while keeping the ventilation with oxygen. The mouse was disconnected time and again to check if it was already breathing spontaneously. In this case, the tube was removed and the mouse put into a cage under an infrared lamp. The whole procedure from induction to emergence of the anaesthesia took 25–35 min.

Concerning pain management, 30–45 min before PAB surgery the mouse received 0.1 mg/kg Buprenorphine (Temgesic, Essex Pharma GmbH, Munich) subcutaneously (SC). For the next 48 h after surgery, the mouse received 0.1 mg/kg buprenorphine SC BID (bis in die) and 2.0 mg/kg carprofen over the drinking water. All mice were checked daily according to a score sheet with a special interest in the development of clinical signs for right heart failure (inactivity, ruffled fur, dyspnoea, and ascites).

Euthanasia took place after haemodynamic measurements; the heart catheter was gently removed from the still anaesthetised mouse before it was sacrificed by incision of the heart to bleed out.

### 2.3 Human material

Human tissue samples of RVs were obtained for routine histological diagnostics. Paraffin sections of seven RV biopsy samples from patients with diagnosed PH were analysed, as well as RV biopsies from three non-PH and non-DCM controls that were investigated for suspected

myocarditis. Tissue that was not needed any more for diagnostic approaches was used for staining in this study. The patients gave informed consent for histological and immunohistological examinations, and the human tissue samples usage was approved by the ethics committee of the University of Tuebingen that conforms the declaration of Helsinki. For further information on patients' characteristics refer [Supplementary material online, Table S1](#).

## 2.4 Statistical analysis

The presented data comprise the means and standard error means (SEM). Significance was determined by one-way analysis of variance (ANOVA) and Newman–Keuls test. The comparison of two groups was analysed by the unpaired *t*-test. Significance was defined as  $P \leq 0.05$ . Statistical details and sample size are indicated in the figure legends. Finally, Pearson correlation coefficients were used for analyses of the correlations.

## 3. Results

### 3.1 Impaired function of RV is accompanied by structural changes

Mice that underwent PAB surgery successfully developed RVH within 3 weeks as determined by RV mass in relation to tibia length (RV/TL, [Supplementary material online, Table S2](#)). Echocardiography revealed an increase in both inner diameter (RVID) and wall thickness (RVWT) of RV in PAB compared with *sham* ([Supplementary material online, Table S2](#)). The relatively thin RV, compared to the left ventricle (LV) that is used to work in a high-pressure system,<sup>24</sup> reacts quickly with a dilatation to the banding of the pulmonary artery. The increase in RVWT additionally demonstrates the development of RVH in our mouse model. The mice did not show any clinical signs for RHF during daily checks. To assess heart function, tricuspid annular plane systolic excursion (TAPSE), and cardiac index (CI) were measured by echocardiography ([Supplementary material online, Table S2](#)). Both parameters were significantly decreased in PAB compared to *sham* animals indicating a deterioration of heart function in PAB mice. Histology revealed an increase in cardiomyocyte size ([Supplementary material online, Table S2](#)) as well as in collagen content in the RV ([Supplementary material online, Table S2](#)) of PAB mice compared to healthy controls. Taken together, these functional and structural data reveal development of RVH in the absence of heart failure in our mouse model of PAB.

### 3.2 Proteasome activity is increased in RVH

The proteolytic activity of the proteasome in RV was determined using luminescent substrates for the  $\beta 1$  and  $\beta 5$  active sites. As depicted in [Figure 1A](#), the caspase like (C-L), as well as the chymotrypsin like (CT-L) activity were significantly increased by more than three-fold in PAB compared to *sham* mice. We confirmed this pronounced increase in proteasomal activity using a second method. The use of activity-based probes (ABP) allows discrimination of several active sites of the proteasome upon binding of a fluorescently labelled probe.<sup>25</sup> This ABP acts like a specific proteasome inhibitor as it covalently binds to the active-site threonine of the catalytic subunits of the proteasome.<sup>26</sup> As such, the extent of binding of the labelled ABP is a direct measure for the number of active sites present and can be quantified for the different catalytic subunits after separation of proteasome complexes by SDS-PAGE ([Figure 1B](#)). ABP

analysis unambiguously confirmed concerted activation of the activity of all three catalytic subunits  $\beta 1$ ,  $\beta 2$ , and  $\beta 5$  in the RV of the PAB mice compared to *sham*. Finally, we have analysed the correlations between the proteolytic activities of the proteasome (C-L and CT-L) and important histological, functional, haemodynamic, and echocardiographic parameters in the *sham* and PAB groups ([Supplementary material online, Figure S13](#)). There was a significant positive correlation between the C-L and CT-L, and several histological and morphometric parameters: cardiomyocyte hypertrophy [ $P = 0.02/r^2 = 0.26$  (C-L and cardiomyocyte size) and  $P = 0.03/r^2 = 0.24$  (CT-L and cardiomyocyte size)]; collagen content [ $P = 0.02/r^2 = 0.28$  (C-L and collagen content) and  $P = 0.005/r^2 = 0.36$  (CT-L and collagen content)]; and RVID [ $P = 0.0008/r^2 = 0.48$  (C-L and RVID) and  $P = 0.002/r^2 = 0.43$  (CT-L and RVID)]. In addition, we noted a significant negative correlation between the C-L and CT-L, and TAPSE [ $P = 0.0009/r^2 = 0.47$  (C-L and TAPSE) and  $P = 0.001/r^2 = 0.45$  (CT-L and TAPSE)]. Finally, there was no correlation between the C-L and CT-L, and systolic blood pressure (SBP).

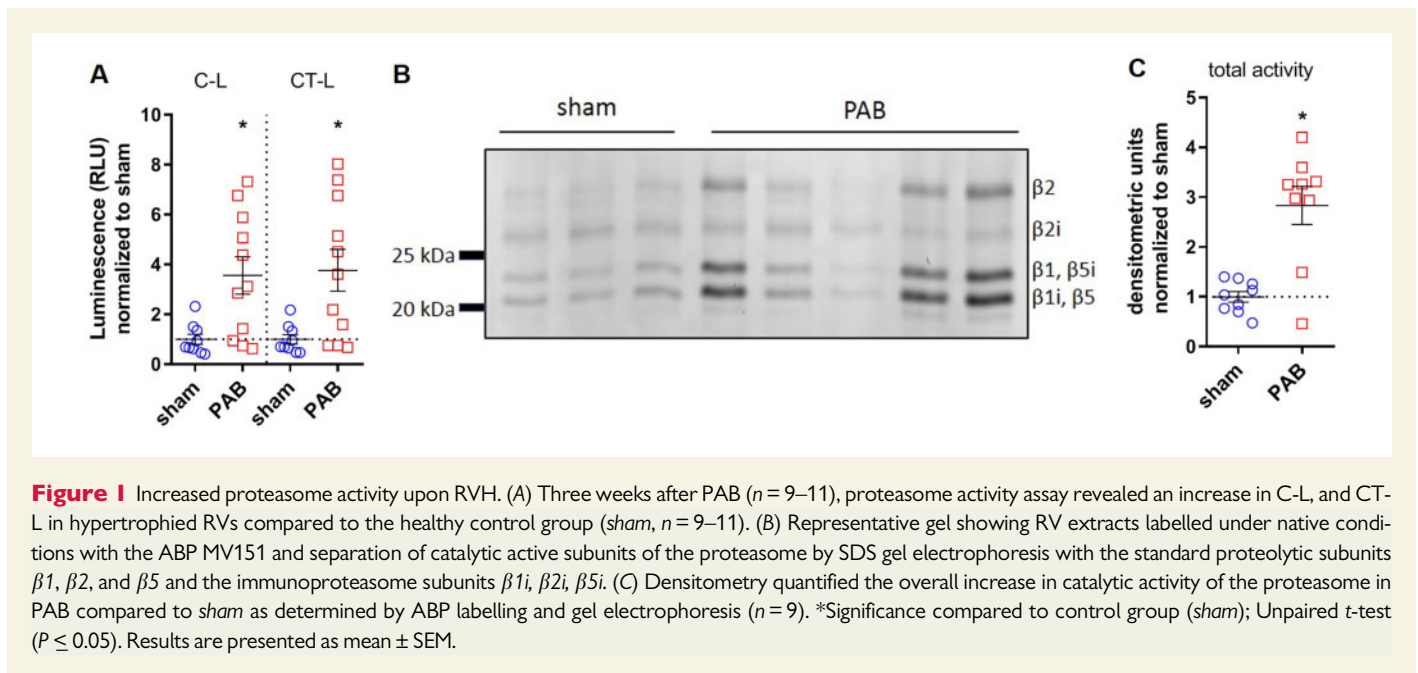
### 3.3 Proteasome inhibition attenuates development of RVH

In order to investigate whether this increase in proteasome activity contributes to the development of RVH in PAB, we applied two distinct proteasome inhibitors. The reversible proteasome inhibitor BTZ has been FDA approved in 2003 as a first generation inhibitor for the treatment of multiple myeloma patients and was used in several preclinical models of human diseases.<sup>27</sup> In contrast, the carfilzomib analogue ONX-0912 represents a second-generation proteasome inhibitor. It is applied orally<sup>28</sup> and binds irreversibly only to the  $\beta 5$  active site of the proteasome.<sup>27</sup>

Preventive treatment of PAB mice twice a week with either BTZ (0.5 mg/kg BW intraperitoneally) or ONX-0912 (50 mg/kg applied by oral gavage) did not significantly alter the ratio of RV mass to tibia length (RV/TL, [Supplementary material online, Figure S2A](#) and [C](#)). In contrast, echocardiography demonstrated significant improvement of RV structure (RVID, [Figure 2A](#) and [C](#)) and function (TAPSE, [Figure 2B](#) and [D](#)), while RV free wall thickness was not altered (RVWT, [Supplementary material online, Figure S2B](#) and [D](#)). The CI ([Supplementary material online, Figure S2E](#) and [G](#)) increased slightly but significantly at constant heart rate (HR, [Supplementary material online, Figure S2F](#) and [H](#)) only in the preventively ONX-treated group. Histology showed that preventive treatment with BTZ led to a reduction of cardiomyocyte size ([Figure 2E](#)), while results did not reach significance in the ONX<sub>prev</sub> group compared with the placebo-treated PAB group ([Figure 2G](#)). Collagen content showed a tendency to decrease in the BTZ and ONX-0912-treated groups compared with the PAB placebo control ([Figure 2F](#) and [H](#)). Constant SBP and diastolic blood pressure ([Supplementary material online, Figure S3](#)) indicated that both proteasome inhibitors had no considerable systemic effects on haemodynamic parameters. However, there was a reduction of SBP in the ONX<sub>prev</sub> group in comparison to the *sham* control ([Supplementary material online, Figure S3C](#)). In summary, these findings suggest that catalytic proteasome inhibition had beneficial effects on RV morphology and function in experimental RVH.

### 3.4 Therapeutic proteasome inhibition reduces RVH

In a next step, we tested both inhibitors for their therapeutic effects on established RVH (BTZ<sub>ther</sub> and ONX<sub>ther</sub>). To confirm development of RVH in our mouse model, we performed echocardiography after 1 week of PAB surgery and compared right heart parameters to



echocardiographic data at baseline (Supplementary material online, Figure S5); PAB mice had already developed pronounced changes in RV structure and function (Supplementary material online, Figure S5). The animals now received either BTZ or ONX-0912 as described above to investigate the possible therapeutic effect of proteasome inhibition on established RVH. Final echocardiography was performed 2 weeks later. CI and HR changed neither in *BTZther* nor in *ONXther* compared to PAB (Supplementary material online, Figure S6E–H). As in the preventive approach, therapeutic treatment with BTZ (*BTZther*) significantly reduced RVID compared to PAB (Figure 3A), while RVWT did not change (Supplementary material online, Figure S6B). In the therapeutic ONX group, proteasome inhibition had beneficial effects on RVH as evidenced by significant reduction of RVID (Figure 3C) and RVWT (Supplementary material online, Figure S6D) compared to PAB. TAPSE improved significantly in both *ONXther* and *BTZther* (Figure 3B and D), but only *ONXther* reduced RV/TL (Supplementary material online, Figure S6C). Treatment with BTZ influenced neither cardiomyocyte size nor collagen content (Figure 3E and F). In contrast, both histopathological parameters were significantly reduced upon the treatment with ONX (Figure 3G and H). Finally, BTZ treatment did not exert any systemic effects on haemodynamic parameters (Supplementary material online, Figure S7). However, there was a reduction of SBP in the *ONXther* group in comparison to the *sham* and PAB controls (Supplementary material online, Figure S7C). This finding has to be taken in consideration in the future studies, as a potential side effect. In summary, these findings suggest that therapeutic application of proteasome inhibitors improved RV structure and function in experimental RVH, with ONX being more effective than BTZ.

### 3.5 26S proteasome activity augmented in RVH

These data support a potential therapeutic value of catalytic proteasome inhibitors in the therapy of RVH. A major drawback of the therapeutic application of proteasome inhibitors, however, are their systemic side effects such as neuropathy<sup>29</sup> and cardiac proteotoxicity.<sup>30</sup> Targeting distinct proteasomal complexes by interfering with the assembly of the 20S

core complex and its proteasome activators was recently proposed as a more specific approach to reduce side effects.<sup>31</sup> In order to better understand proteasome activation in RVH, we analysed the formation of proteasome complexes in the right heart of PAB mice compared to healthy controls. Western blot analysis and subsequent densitometry revealed increased levels of the catalytic subunit  $\beta 1$  as well as of subunit  $\alpha 3$  (Figure 4A) in PAB mice. Moreover, expression of the 19S regulatory subunits Rpt5 and Rpn6 was also clearly elevated in the hypertrophied RV of PAB mice (Figure 4A). These findings were accompanied by augmented activity of singly and doubly capped 26S proteasome complexes as revealed by labelling of active proteasome complexes in native gels using the aforementioned ABPs (Figure 4B). Enhanced 26S proteasome activity was associated with increased turnover of ubiquitinated substrates as indicated by elevated levels of K48-polyubiquitinated proteins (Figure 4A). These data indicate that an elevation in proteasomal activity is due to an increased activity of the 26S proteasomes which mediate ubiquitin-dependent protein degradation in the hypertrophied RV.<sup>12</sup>

### 3.6 Rpn6 increased in hypertrophied RV tissue

We corroborated our data by focusing on the cell-specific expression of the 19S subunit Rpn6 in hypertrophied RV. Recent publications have identified Rpn6 as a major regulator for the assembly and activation of the 26S proteasome complexes.<sup>32</sup> Cell-specific expression of Rpn6 in diseased tissue may be used as a surrogate marker for elevated 26S proteasome activity.<sup>33</sup> Immunohistochemical staining for Rpn6 in the RV of *sham* and PAB mice revealed co-localization of Rpn6 (red colour) with tropomyosin (brown colour), indicating expression of Rpn6 in the cytoplasm of cardiomyocytes (Figure 5A). The staining of both Rpn6 and tropomyosin was patchy in the *sham* group. However, in the PAB group, Rpn6 as well as tropomyosin immunostaining revealed more diffuse distribution in the cytoplasm of cardiomyocytes, which might be indicative of disease-associated phenotypic alterations of cardiomyocytes following PAB. We observed an increase in Rpn6 staining in RVH of PAB mice compared to healthy tissue of *sham* mice, which goes in line with our

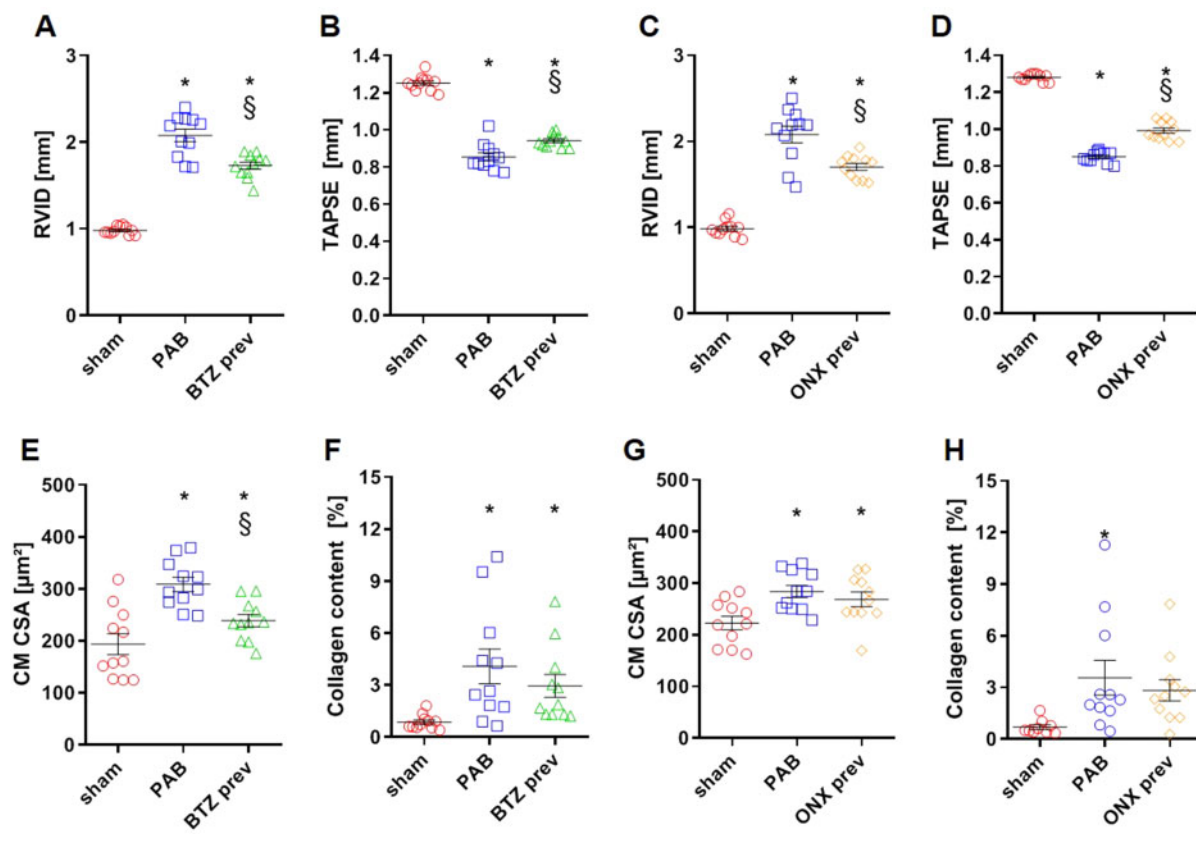


**Figure 2** Preventive proteasome inhibition partly improved function and structure of RV. (A, C) Three weeks after PAB, preventive proteasome inhibition by Bortezomib (BTZ<sub>prev</sub>,  $n = 9-11$ ) and ONX (ONX<sub>prev</sub>,  $n = 9-11$ ) significantly reduced the RVID compared to the placebo-treated group (PAB,  $n = 9-11$ ). (B, D) Both proteasome inhibitors significantly increased right ventricular function as determined by TAPSE. (E, G) Preventive proteasome inhibition with Bortezomib (BTZ<sub>prev</sub>) but not ONX (ONX<sub>prev</sub>) resulted in a decrease in CM CSA compared to placebo-treated PAB controls. (F, H) Analysis of the collagen content revealed a slight decrease in PAB mice treated with proteasome inhibitors. Staining with WGA-FITC for cardiomyocyte size measurement and Sirius Red for collagen detection see [Supplementary material online, Figure S4](#). §Significance compared to placebo-treated PAB group ( $n = 9-11$ ). \*Significance compared to healthy control group (sham,  $n = 9-11$ ); One-way ANOVA with Newman-Keuls test ( $P \leq 0.05$ ). Results are presented as mean  $\pm$  SEM.

quantitative western blot data for Rpn6. These data suggest that elevated expression of Rpn6 contributes to increased 26S proteasome activity in hypertrophied cardiomyocytes in mice. In order to apply this finding to human RVH, we stained biopsies of RV tissue obtained from patients with RV cardiomyopathies for Rpn6 (Figure 5B). Of note, Rpn6 (pale red colour) expression was again co-localized to cardiomyocytes and it was significantly elevated in hypertrophied heart tissue of patients with RVH (Figure 5C). Interestingly, in humans, expression of Rpn6 was only faint in tropomyosin (dark red colour) expressing cardiomyocytes of normal heart tissue, whereas it was eminently induced throughout the cytoplasm of tropomyosin-positive cardiomyocytes of hearts from patients with RVH.

### 3.7 Effects of BTZ treatment on proteostasis and inflammatory signalling in RVH

BTZ treatment did not result in accumulation of K48-linked polyubiquitinated proteins in the RV tissue, as compared to the control group (PAB) ([Supplementary material online, Figure S11A](#)). In addition, there was no

induction of autophagy upon the treatment with BTZ (LC3B) ([Supplementary material online, Figure S11B](#)). However, the application of BTZ significantly increased the expression of I $\kappa$ B $\alpha$ , in comparison to the PAB control ([Supplementary material online, Figure S11B](#)).

## 4. Discussion

### 4.1 Proteasome inhibition partially reduces RVH

Despite the success of proteasome inhibition in the field of haematopoietic tumours, severe side effects were reported since the first approval of BTZ in 2003 as third treatment of multiple myeloma.<sup>34</sup> Application over a longer period resulted in accumulation of misfolded and non-sense proteins.<sup>34</sup> From research on BTZ, neuropathies were well-known,<sup>29</sup> but case reports described also signs of cardiac toxicity after the treatment with both reversible<sup>30,35</sup> and irreversible<sup>36</sup> proteasome inhibitors which reversed upon termination of therapy.<sup>37</sup> This was taken into consideration when designing this study by choosing a sequential design to adjust the right dose and administering both proteasome

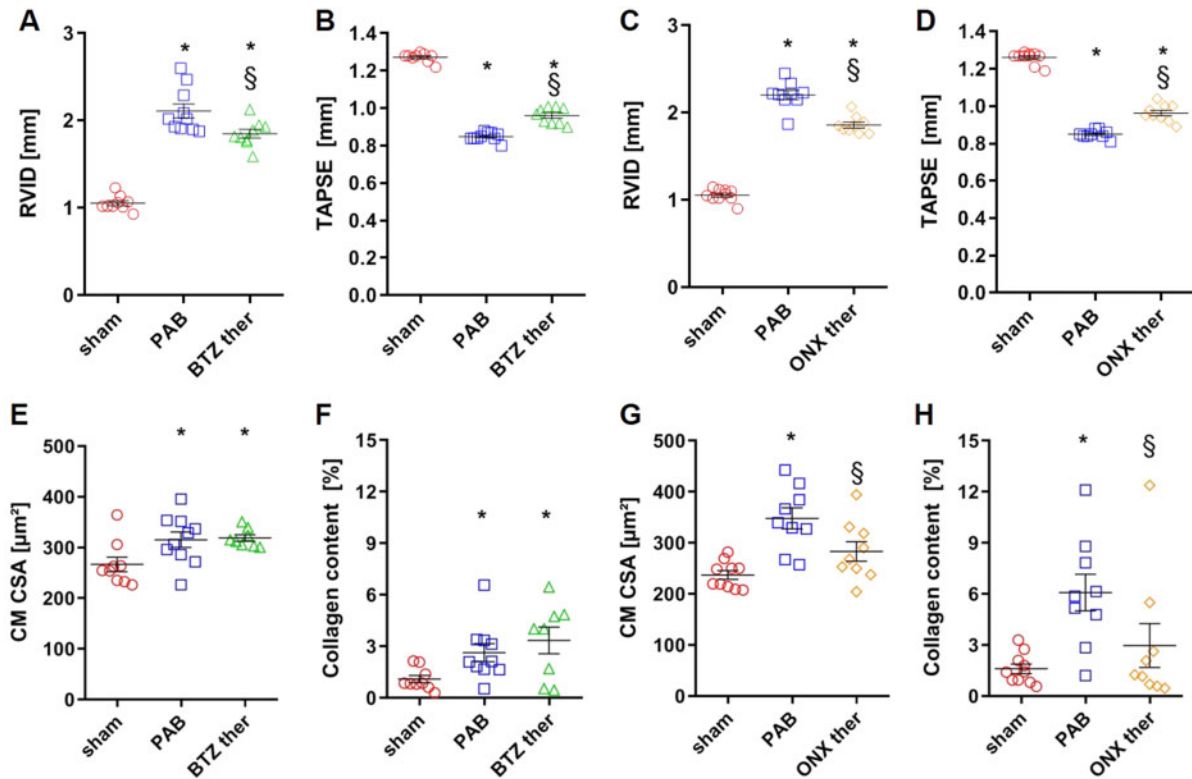
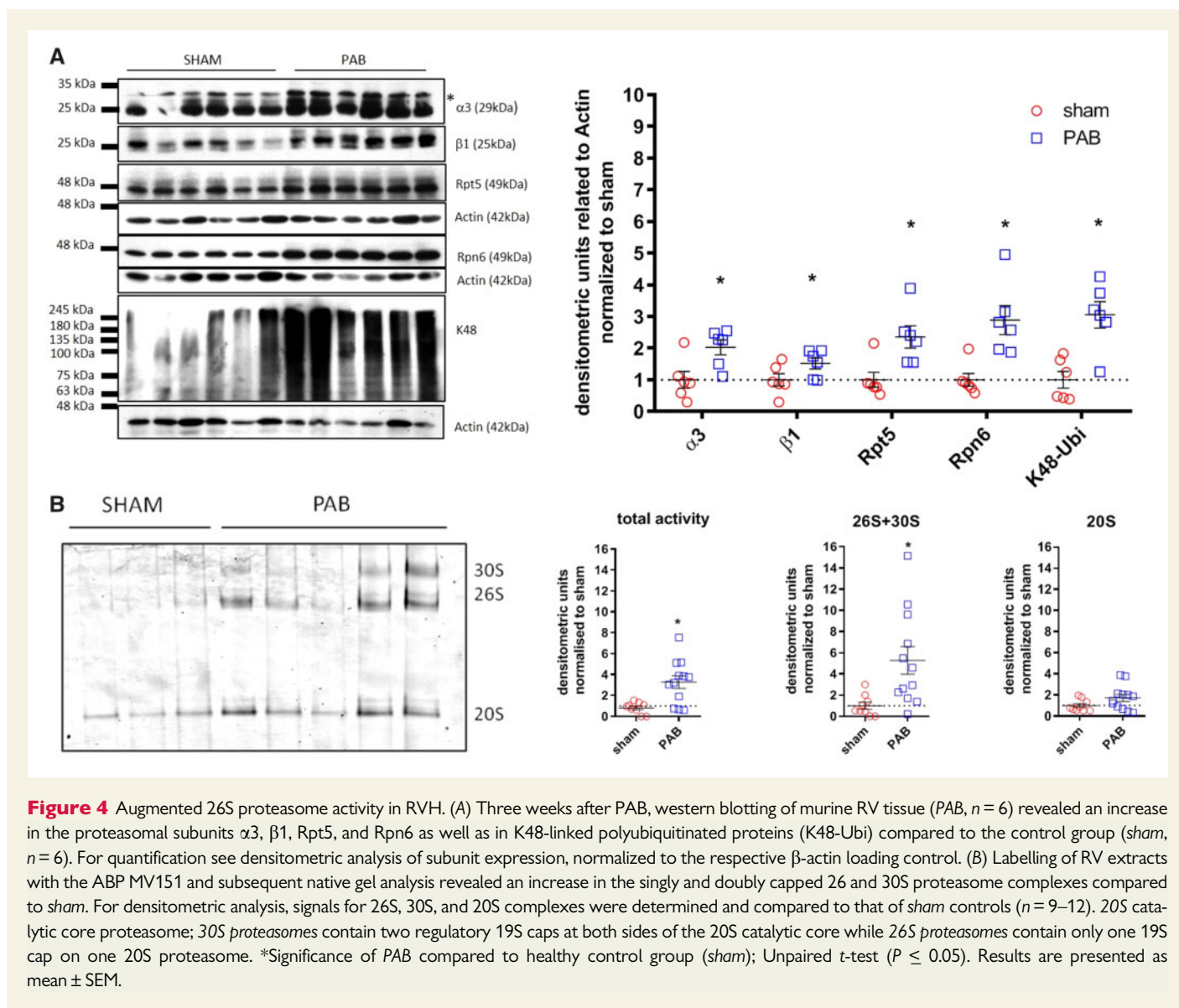


**Figure 3** Therapeutic proteasome inhibition reduced experimental RVH. (A, C) Three weeks after PAB, therapeutic proteasome inhibition by Bortezomib (BTZ<sub>ther</sub>,  $n = 8-10$ ), and ONX (ONX<sub>ther</sub>,  $n = 8-10$ ) significantly reduced the RVID compared to the placebo-treated control group (PAB,  $n = 8-10$ ). (B, D) Both proteasome inhibitors significantly increased right ventricular function as determined by TAPSE. (E, G) Therapeutic proteasome inhibition with ONX (ONX<sub>ther</sub>,  $n = 8-10$ ) but not BTZ (BTZ<sub>ther</sub>,  $n = 8-10$ ) led to a significant decrease in CM CSA compared to placebo-treated PAB controls (PAB,  $n = 8-10$ ). (F, H) Collagen content significantly decreased in RV that had been treated therapeutically with ONX (ONX<sub>ther</sub>,  $n = 8-10$ , H), but not in BTZ-treated RV (BTZ<sub>ther</sub>,  $n = 8-10$ , F). Staining with WGA-FITC for cardiomyocyte size measurement and Sirius Red for collagen detection see [Supplementary material online, Figure S8](#). §Significance compared to placebo-treated control group (PAB,  $n = 8-10$ ). \*Significance compared to healthy control group (sham,  $n = 8-10$ ); One-way ANOVA with Newman–Keuls test ( $P \leq 0.05$ ). Results are presented as mean  $\pm$  SEM.

inhibitors only twice weekly. We carefully chose inhibitor doses that were non-toxic and would allow prolonged and repeated treatment without inducing any off-target effect. Several reports applied BTZ in mice at higher doses and for longer time points without observing toxic-side effects.<sup>38-40</sup> Regarding the dosing of ONX, we applied a low dose and repetitive dosing based on data from our lab and others.<sup>41,42</sup>

The groups of Hedhli<sup>43</sup> and Stansfield<sup>44</sup> had reported that proteasome inhibition in experimental LVH not only decreased, but also prevented cardiac remodelling. Our data for RVH provide evidence that treatment with BTZ or ONX only partially improves RV function and structure, suggesting that partial proteasome inhibition in the beginning of RVH may at least delay the development of RHF. Proteasome inhibitors have also been shown to exert anti-fibrotic effects in hearts at non-toxic doses.<sup>45</sup> It is thus well feasible that slightly reduced fibrotic remodelling as observed in our PAB model of RVH contributes to the overall protective effects of BTZ and ONX in our study. On the molecular level, the applied inhibitor doses did not induce pronounced accumulation of polyubiquitinated proteins in the RV ([Supplementary material online, Figure S11A](#)) and also did not result in a compensatory induction of autophagy ([Supplementary material online, Figure S11B](#)),<sup>46</sup> suggesting that indeed the proteasome is only partially inhibited. The beneficial

effects of partial proteasome inhibition have previously been discussed.<sup>14</sup> Of note, BTZ treatment induced accumulation of the NF- $\kappa$ B inhibitor I $\kappa$ B $\alpha$ —but not I $\kappa$ B $\beta$ —in the RVs of BTZ-treated mice indicating suppression of inflammatory NF- $\kappa$ B signalling, a well-established effect of proteasome inhibition ([Supplementary material online, Figure S11B](#)).<sup>47</sup> It is tempting to speculate that this reduced activation of NF- $\kappa$ B contributes to the anti-hypertrophic effects of BTZ in our study, as suggested for left heart hypertrophy.<sup>48,49</sup> Interestingly, we observed that ONX was more efficient in recovering RVH function and structure than BTZ. This effect might be related to the distinct pharmacologic features of the boronate inhibitor BTZ and the  $\alpha$ ,  $\beta$ -epoxyketone inhibitor ONX-0912.<sup>50</sup> While BTZ reversibly inhibits both the chymotrypsin- and caspase-like activity, ONX-0912 is selective for the chymotrypsin-like activity which it inhibits irreversibly.<sup>29</sup> Moreover, off-target effects have been described for BTZ but are not evident for the ONX-0912 analogue carfilzomib which has also recently been approved for treatment of multiple myeloma.<sup>29</sup> These distinct pharmacological features of the two applied proteasome inhibitors BTZ and ONX-0912 may thus account for the observed effects as supported by our previous comparative study on lung fibrosis.<sup>41</sup> A comparative analysis on the therapeutic effects of reversible vs. irreversible proteasome inhibitors on heart function, like in



our study, has not been performed before and adds to the understanding of the differential effects of distinct proteasome inhibitors.<sup>14</sup>

## 4.2 Proteasome activity increased in RVH

We provide evidence that the catalytic activity of the proteasome increases in experimental RVH. This is in contrast to two other studies reporting a decrease in proteasome function; Rajagopalan *et al.*<sup>51</sup> observed that proteasome activity was decreased in mice with PAB induced RVH. This was associated with up-regulation of key regulators for the UPS such as several E3 ligases and the 19S subunit Rpt5. Fessart *et al.*<sup>22</sup> also observed an impairment of the proteasome system in rats with hypoxia- or monocrotaline-induced RVH. Importantly, both studies analysed animals that had developed clinical signs of RHF in contrast to our model of RVH. We thus hypothesize that proteasome function in RVH vs. RHF is related to the extent of maladaptive cardiac remodelling. This has also been suggested for the left heart: in TAC-induced left heart hypertrophy, Ranek *et al.*<sup>52</sup> observed an increase in the activity of the proteasome within 2 weeks. Heart function and proteasome activity,

however, deteriorated within the following weeks until heart failure eventuated. Tsukamoto *et al.*<sup>53</sup> corroborated this finding in experimental LVH and in LVH samples of patients with heart failure. These data indicate that the activity of the proteasome is related to the stage of myocardial remodelling with enhanced activity upon adaptive hypertrophic remodelling and loss of proteasome function accompanying progressive heart failure. We propose that this concept also holds true for right heart remodelling; adaptive RVH is accompanied by an increase in proteasomal activity, whereas at later stage of maladaptive cardiac remodelling not only heart but also proteasome function deteriorates. Accordingly, proteasome inhibitors may have opposite effects, depending on the stage of cardiac remodelling. During adaptive cardiac remodelling they act protective and even reverse right and left heart remodelling, while at maladaptive remodelling catalytic proteasome inhibitors will have detrimental effects. Any further inhibition of the proteasome will then result in cardiac proteotoxicity and provoke a hypertrophied right heart to fail.<sup>52</sup> According to this concept, determination of proteasome activity in RV or LV biopsies emerge as a novel discriminating marker for defining progressive stages of heart dysfunction with the potential to

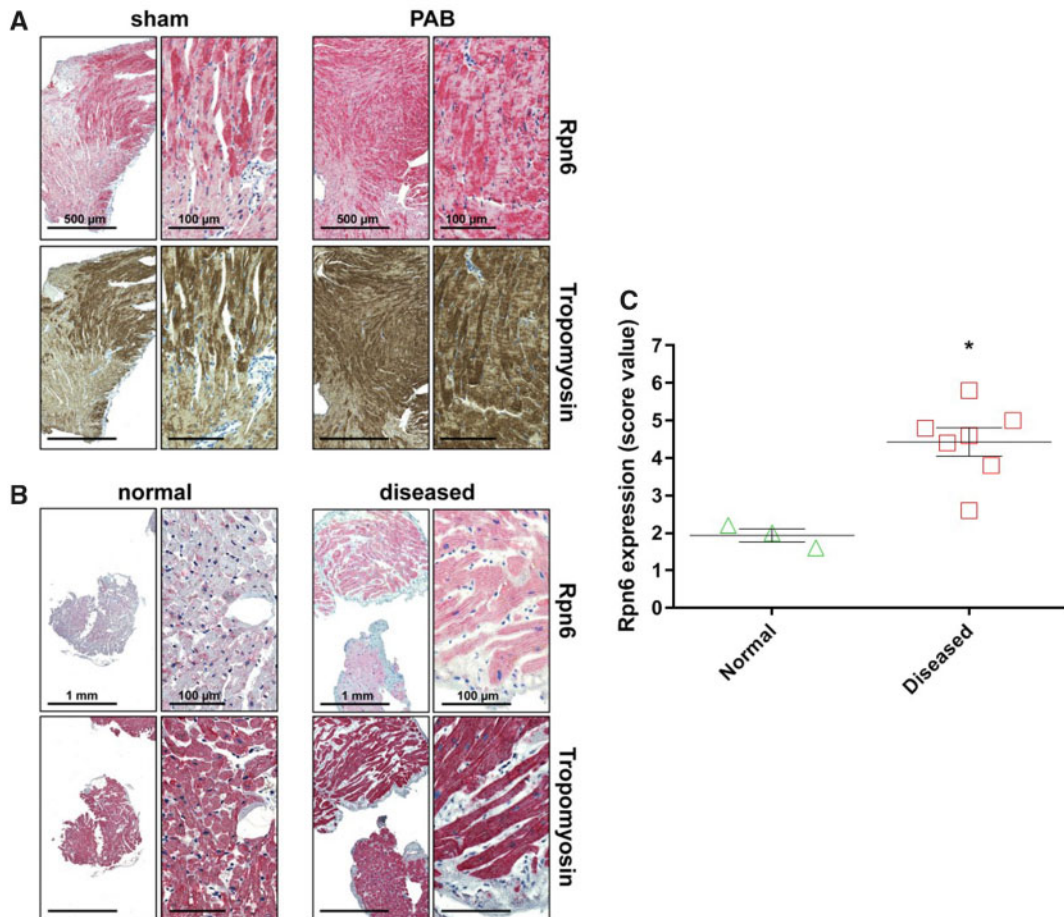


**Figure 5** Expression of Rpn6 in normal and diseased hearts of (A) mice and (B) humans. (A) PAB was used to induce RVH in mice. Mice with RVH revealed cytoplasmic overexpression of Rpn6 in cardiomyocytes (red stain, upper row) which were identified in a parallel section with the cell-specific marker protein tropomyosin (brown stain, lower row). (B) Tropomyosin-expressing cardiomyocytes (dark red stain, lower row) from patients with RVH showed diffuse cytoplasmic overexpression of Rpn6 (pale red stain, upper row) as compared to normal hearts. (C) Semi-quantitative analysis of Rpn6 expression in human samples is shown. Unpaired t-test ( $P \leq 0.05$ ). Results are presented as mean  $\pm$  SEM ( $n = 3-7$ ).

define a personalized therapeutic regimen for patients with PH or cardiomyopathies.

### 4.3 Increased assembly of the 26S proteasome in RVH

Our analysis of proteasome expression and function revealed that the increased proteasome activity in hypertrophied RV can be ascribed to augmented formation and activity of 26S proteasome complexes. Activation of 26S proteasomes was accompanied by an increased turnover of polyubiquitinated substrates as shown previously.<sup>8</sup> This finding is also in line with the recently described positive feedback of the mTOR pathway to the proteasome that links increased protein synthesis to activation of proteasomal protein degradation.<sup>54</sup> In this study, Zhang et al.<sup>54</sup> demonstrated mTOR-dependent transcriptional activation of the proteasome via the transcription factor Nrf1. In contrast, we were unable to observe concerted induction of proteasomal gene expression on the mRNA level. The only proteasomal gene that we found transcriptionally activated in experimental RVH was the 19S regulatory subunit Rpn6 (Supplementary material online, Figure S9). Of note, this subunit has

been proposed to act as a structural clamp that stabilizes the interaction of the 19S regulatory complex with the 20S catalytic core.<sup>55</sup> In line with these structural data, Rpn6 has been identified as a rate-limiting subunit for regulating assembly of 26S proteasomes in differentiating embryonic stem cells and myofibroblasts.<sup>32,33</sup> The particular role of Rpn6 for the activation of 26S proteasome function is also supported by the recent observation that phosphorylation of Rpn6 by protein kinase A enhances assembly of 26S proteasome complexes.<sup>56</sup> Taken together, these data strongly support the notion that Rpn6 is a potential marker for enhanced 26S proteasome activity. In line with this concept, increased 26S proteasome activity was accompanied by Rpn6 overexpression in hypertrophied RVs of PAB mice with predominant localization to hypertrophied cardiomyocytes as determined by quantitative western blot and semi-quantitative immunohistochemistry analysis. We also observed Rpn6 to be highly expressed in hypertrophied cardiomyocytes in RV of human patients. This finding opens the possibility that immunohistochemical detection of Rpn6 might be used as a surrogate biomarker for elevated proteasome activity in order to discriminate progressive stages of heart dysfunction as proposed above.

Moreover, identification of Rpn6 as an important regulator for 26S proteasome activity suggests that this subunit might serve as a novel distinct target to specifically interfere with 26S proteasome activation. Indeed, genetically induced overexpression of Rpn6 conferred resistance of *Caenorhabditis elegans* worms to proteotoxic stress.<sup>57</sup> Conversely, silencing of Rpn6 altered differentiation of human embryonic stem cells<sup>32</sup> and counteracted TGF $\beta$ -induced myodifferentiation of human lung fibroblasts.<sup>33</sup> These studies suggest that targeting the assembly of the 19S complex via Rpn6 might provide a more specific approach to interfere with hypertrophy-associated 26S proteasome activation compared to the indiscriminate inhibition of all proteasome complexes using catalytic proteasome inhibitors.

## 5. Conclusion

Our study revealed that

- proteasome expression and activities increased in experimental RVH,
- proteasome inhibition had beneficial therapeutic effects on RVH with ONX-0912 being more potent than BTZ, and
- 26S proteasome formation increased via the regulatory unit Rpn6, making Rpn6 a more specific target for proteasome interference than catalytic inhibition.

To the best of our knowledge, we provide for the first time evidence that there is an up-regulation of Rpn6 in experimental RVH. Moreover, Rpn6 was found when investigating RV tissue of human hypertrophied hearts, indicating the relevance of this animal model to the human situation. Future investigations can focus on Rpn6 as new, more specific therapeutic target for proteasome interference.

## Supplementary material

Supplementary material is available at *Cardiovascular Research* online.

## Acknowledgements

The authors would like to thank Herman Overkleft for sharing the activity-based probes with us.

**Conflict of interest:** none declared.

## Funding

This study was supported by the Universities of Giessen and Marburg Lung Center (UGMLC), by intramural funds of the Helmholtz Zentrum München and by funding of the German Center for Lung Research (DZL).

## References

1. Thenappan T, Gombert-Maitland M. Epidemiology of pulmonary hypertension and right ventricular failure in left heart failure. *Curr Heart Fail Rep* 2014;**11**:428–435.
2. Ryan JJ, Tedford RJ. Diagnosing and treating the failing right heart. *Curr Opin Cardiol* 2015;**30**:292–300.
3. Stenmark KR, Meyrick B, Galie N, Mooi WJ, McMurtry IF. Animal models of pulmonary arterial hypertension: the hope for etiological discovery and pharmacological cure. *Am J Physiol Lung Cell Mol Physiol* 2009;**297**:L1013–L1032.
4. Bogaard HJ, Abe K, Vonk Noordegraaf A, Voelkel NF. The right ventricle under pressure. *Chest* 2009;**135**:794–804.
5. Schermuly RT, Ghofrani HA, Wilkins MR, Grimminger F. Mechanisms of disease: pulmonary arterial hypertension. *Nat Rev Cardiol* 2011;**8**:443–455.
6. Vonk-Noordegraaf A, Haddad F, Chin KM, Forfia PR, Kawut SM, Lumens J, Naeije R, Newman J, Oudiz RJ, Provencher S, Torbicki A, Voelkel NF, Hassoun PM. Right heart adaptation to pulmonary arterial hypertension: physiology and pathobiology. *J Am Coll Cardiol* 2013;**62**:D22–D33.
7. Walker LA, Buttrick PM. The right ventricle: biologic insights and response to disease: updated. *Curr Cardiol Rev* 2013;**9**:73–81.
8. Mearini G, Schlossarek S, Willis MS, Carrier L. The ubiquitin-proteasome system in cardiac dysfunction. *Biochim Biophys Acta* 2008;**1782**:749–763.
9. Hershko A, Ciechanover A. The ubiquitin system. *Annu Rev Biochem* 1998;**67**:425–479.
10. Groll M, Ditzel L, Löwe J, Stock D, Bochtler M, Bartunik HD, Huber R. Structure of 20S proteasome from yeast at 2.4 Å resolution. *Nature* 1997;**386**:463–471.
11. Stadtmueller BM, Hill CP. Proteasome activators. *Mol Cell* 2011;**41**:8–19.
12. Meiners S, Keller IE, Semren N, Caniard A. Regulation of the proteasome: evaluating the lung proteasome as a new therapeutic target. *Antioxid Redox Signal* 2014;**21**:2364–2382.
13. Lander GC, Martin A, Nogales E. The proteasome under the microscope: the regulatory particle in focus. *Curr Opin Struct Biol* 2013;**23**:243–251.
14. Meiners S, Ludwig A, Stangl V, Stangl K. Proteasome inhibitors: poisons and remedies. *Med Res Rev* 2008;**28**:309–327.
15. Schmidt M, Finley D. Regulation of proteasome activity in health and disease. *Biochim Biophys Acta* 2014;**1843**:13–25.
16. Gomes AV, Zong C, Edmondson RD, Li X, Stefani E, Zhang J, Jones RC, Thyparambil S, Wang GW, Qiao X, Bardag-Gorce F, Ping P. Mapping the murine cardiac 26S proteasome complexes. *Circ Res* 2006;**99**:362–371.
17. Predmore JM, Wang P, Davis F, Bartolone S, Westfall MV, Dyke DB, Pagani F, Powell SR, Day SM. Ubiquitin proteasome dysfunction in human hypertrophic and dilated cardiomyopathies. *Circulation* 2010;**121**:997–1004.
18. Drews O. The left and right ventricle in the grip of protein degradation: similarities and unique patterns in regulation. *J Mol Cell Cardiol* 2014;**72**:52–55.
19. Gavazzoni M, Vizzardelli E, Gorga E, Bonadei I, Rossi L, Belotti A, Rossi G, Ribolla R, Metra M, Raddino R. Mechanism of cardiovascular toxicity by proteasome inhibitors: new paradigm derived from clinical and pre-clinical evidence. *Eur J Pharmacol* 2018;**828**:80–88.
20. Herrmann J, Wohlert C, Saguner AM, Flores A, Nesbitt LL, Chade A, Lerman LO, Lerman A. Primary proteasome inhibition results in cardiac dysfunction. *Eur J Heart Fail* 2013;**15**:614–623.
21. Wang X, Ibrahim YF, Das D, Zungu-Edmondson M, Shults NV, Suzuki YJ. Carfilzomib reverses pulmonary arterial hypertension. *Cardiovasc Res* 2016;**110**:188–199.
22. Fessart D, Martin-Negrier ML, Claverol S, Thiolat ML, Crevel H, Toussaint C, Bonneau M, Muller B, Savineau JP, Delom F. Proteomic remodeling of proteasome in right heart failure. *J Mol Cell Cardiol* 2014;**66**:41–52.
23. Shi L, Kojonazarov B, Elgheznawy A, Popp R, Dahal BK, Böhm M, Pullamsetti SS, Ghofrani HA, Gödecke A, Jungmann A, Katus HA, Müller OJ, Schermuly RT, Fisslthaler B, Seeger WW, Fleming I. miR-223-IGF-IR signaling in hypoxia- and load-induced right ventricular failure: a novel therapeutic approach. *Cardiovasc Res* 2016;**111**:184–193.
24. Apostolakis S, Konstantinides S. The right ventricle in health and disease: insights into physiology, pathophysiology and diagnostic management. *Cardiology* 2012;**121**:263–273.
25. Verdoes M, Florea BI, Menendez-Benito V, Maynard CJ, Witte MD, van der Linden WA, van den Nieuwendijk AM, Hofmann T, Berkens CR, van Leeuwen FW, Groothuis TA, Leeuwenburgh MA, Ovaia H, Neeffes JJ, Filipov DV, van der Marel GA, Dantuma NP, Overkleft HS. A fluorescent broad-spectrum proteasome inhibitor for labeling proteasomes *in vitro* and *in vivo*. *Chem Biol* 2006;**13**:1217–1226.
26. Cravatt BF, Wright AT, Kozarich JW. Activity-based protein profiling: from enzyme chemistry to proteomic chemistry. *Annu Rev Biochem* 2008;**77**:383–414.
27. Dick LR, Fleming PE. Building on bortezomib: second-generation proteasome inhibitors as anti-cancer therapy. *Drug Discov Today* 2010;**15**:243–249.
28. Obrist F, Manic G, Kroemer G, Vitale I, Galluzzi L. Trial watch: proteasomal inhibitors for anticancer therapy. *Mol Cell Oncol* 2015;**2**:e974463.
29. Huber EM, Heinemeyer WW, Groll M. Bortezomib-resistant mutant proteasomes: structural and biochemical evaluation with carfilzomib and ONX 0914. *Structure* 2015;**23**:407–417.
30. Bockorny M, Chakravarty S, Schulman P, Bockorny B, Bona R. Severe heart failure after bortezomib treatment in a patient with multiple myeloma: a case report and review of the literature. *Acta Haematol* 2012;**128**:244–247.
31. Gaczynska M, Osmulski P. Targeting protein-protein interactions in the proteasome super-assemblies. *Curr Top Med Chem* 2015;**15**:2056–2067.
32. Vilchez D, Boyer L, Morante I, Lutz M, Merkwirth C, Joyce D, Spencer B, Page L, Masliah E, Berggren WT, Gage FH, Dillin A. Increased proteasome activity in human embryonic stem cells is regulated by PSMD11. *Nature* 2012;**489**:304–308.
33. Semren N, Welk V, Korfei M, Keller IE, Fernandez IE, Adler H, Günther A, Eickelberg O, Meiners S. Regulation of 26S proteasome activity in pulmonary fibrosis. *Am J Respir Crit Care Med* 2015;**192**:1089–1101.
34. Adams J. The development of proteasome inhibitors as anticancer drugs. Review. *Cancer Cell* 2004;**5**:417–421.

35. Voortman J, Giaccone G. Severe reversible cardiac failure after bortezomib treatment combined with chemotherapy in a non-small cell lung cancer patient: a case report. *BMC Cancer* 2006;**6**:129.
36. Hasinoff BB, Patel D, Wu X. Molecular mechanisms of the cardiotoxicity of the proteasomal-targeted drugs bortezomib and carfilzomib. *Cardiovasc Toxicol* 2017;**17**: 237–250.
37. Grandin EW, Ky B, Cornell RF, Carver J, Lenihan DJ. Patterns of cardiac toxicity associated with irreversible proteasome inhibition in the treatment of multiple myeloma. *J Card Fail* 2015;**21**:138–144.
38. Manning ML, Mason-Osann E, Onda M, Pastan I. Bortezomib reduces pre-existing antibodies to recombinant immunotoxins in mice. *J Immunol* 2015;**194**:1695–1701.
39. Wagner-Ballon O, Pisani DF, Gastinne T, Tulliez M, Chaligne R, Lacout C, Aurade F, Villeval JL, Gonin P, Vainchenker W, Giraudier S. Proteasome inhibitor bortezomib impairs both myelofibrosis and osteosclerosis induced by high thrombopoietin levels in mice. *Blood* 2007;**110**:345–353.
40. Zeniya M, Mori T, Yui N, Nomura N, Mandai S, Isobe K, Chiga M, Sohara E, Rai T, Uchida S. The proteasome inhibitor bortezomib attenuates renal fibrosis in mice via the suppression of TGF- $\beta$ 1. *Sci Rep* 2017;**7**:13086.
41. Semren N, Habel-Ungewitter NC, Fernandez IE, Königshoff M, Eickelberg O, Stöger T, Meiners S. Validation of the 2nd generation proteasome inhibitor oprozomib for local therapy therapy of pulmonary fibrosis. *PLoS One* 2015;**10**:e0136188.
42. Chauhan D, Singh AV, Aujay M, Kirk CJ, Bandi M, Ciccarelli B, Rajee N, Richardson P, Anderson KC. A novel orally active proteasome inhibitor ONX 0912 triggers *in vitro* and *in vivo* cytotoxicity in multiple myeloma. *Blood* 2010;**116**:4906–4915.
43. Hedhli N, Lizano P, Hong C, Fritzky LF, Dhar SK, Liu H, Tian Y, Gao S, Madura K, Vatner SF, Depre C. Proteasome inhibition decreases cardiac remodeling after initiation of pressure overload. *Am J Physiol Heart Circ Physiol* 2008;**295**:H1385–H1393.
44. Stansfield WE, Tang RH, Moss NC, Baldwin AS, Willis MS, Selzman CH. Proteasome inhibition promotes regression of left ventricular hypertrophy. *Am J Physiol Heart Circ Physiol* 2008;**294**:H645–H650.
45. Meiners S, Hoher B, Weller A, Laule M, Stangl V, Guenther C, Godes M, Mrozikiewicz A, Baumann G, Stangl K. Downregulation of matrix metalloproteinases and collagens and suppression of cardiac fibrosis by inhibition of the proteasome. *Hypertension* 2004;**44**:471–477.
46. Korolchuk VI, Menzies FM, Rubinsztein DC. Mechanisms of cross-talk between the ubiquitin-proteasome and autophagy-lysosome systems. *FEBS Lett* 2010;**584**: 1393–1398.
47. Yamamoto Y, Gaynor RB. Therapeutic potential of inhibition of the NF-kappaB pathway in the treatment of inflammation and cancer. *J Clin Invest* 2001;**107**:135–142.
48. Purcell NH, Tang G, Yu C, Mercurio F, DiDonato JA, Lin A. Activation of NF-kappa B is required for hypertrophic growth of primary rat neonatal ventricular cardiomyocytes. *Proc Natl Acad Sci USA* 2001;**98**:6668–6673.
49. Gupta S, Young D, Sen S. Inhibition of NF-kappaB induces regression of cardiac hypertrophy, independent of blood pressure control, in spontaneously hypertensive rats. *Am J Physiol Heart Circ Physiol* 2005;**289**:H20–H29.
50. Dou QP, Zonder JA. Overview of proteasome inhibitor-based anti-cancer therapies: perspective on bortezomib and second generation proteasome inhibitors versus future generation inhibitors of ubiquitin-proteasome system. *Curr Cancer Drug Targets* 2014;**14**:517–536.
51. Rajagopalan V, Zhao M, Reddy S, Fajardo G, Wang X, Dewey S, Gomes AV, Bernstein D. Altered ubiquitin-proteasome signaling in right ventricular hypertrophy and failure. *Am J Physiol Heart Circ Physiol* 2013;**305**:H551–H562.
52. Ranek MJ, Zheng H, Huang W, Kumarapeli AR, Li J, Liu J, Wang X. Genetically induced moderate inhibition of 20S proteasomes in cardiomyocytes facilitates heart failure in mice during systolic overload. *J Mol Cell Cardiol* 2015;**85**:273–281.
53. Tsukamoto O, Minamino T, Okada K, Shintani Y, Takashima S, Kato H, Liao Y, Okazaki H, Asai M, Hirata A, Fujita M, Asano Y, Yamazaki S, Asanuma H, Hori M, Kitakaze M. Depression of proteasome activities during the progression of cardiac dysfunction in pressure-overloaded heart of mice. *Biochem Biophys Res Commun* 2006; **340**:1125–1133.
54. Zhang Y, Nicholatos J, Dreier JR, Ricoult SJ, Widenmaier SB, Hotamisligil GS, Kwiatkowski DJ, Manning BD. Coordinated regulation of protein synthesis and degradation by mTORC1. *Nature* 2014;**513**:440–443.
55. Pathare GR, Nagy I, Bohn S, Unverdorben P, Hubert A, Körner R, Nickell S, Lasker K, Sali A, Tamura T, Nishioka T, Förster F, Baumeister W, Bracher A. The proteasomal subunit Rpn6 is a molecular clamp holding the core and regulatory subcomplexes together. *Proc Natl Acad Sci USA* 2012;**109**:149–154.
56. Lokireddy S, Kukushkin NV, Goldberg AL. cAMP-induced phosphorylation of 26S proteasomes on Rpn6/PSMD11 enhances their activity and the degradation of misfolded proteins. *Proc Natl Acad Sci USA* 2015;**112**:85.
57. Vilchez D, Morante I, Liu Z, Douglas PM, Merkwirth C, Rodrigues AP, Manning G, Dillin A. RPN-6 determines *C. elegans* longevity under proteotoxic stress conditions. *Nature* 2012;**489**:263–268.